JOURNAL OF MATERIALS SCIENCE 32 (1997) 1221–1227

Effects of alloying elements on the electrochemical characteristics of iron aluminides

H. C. CHOE
Department of Iron Manufacture and Metallurgical Engineering, Kwang Yang College, Kwang Yang, 545-800, Korea

H. S. KIM
Department of Materials Science and Metallurgical Engineering, Sunchoen National University, Sunchoen, 540-742, Korea

D. C. CHOI, K. H. KIM
Department of Metallurgical Engineering, Chonnam National University, Kwangju, 500-757, Korea

Effects of alloying elements on the electrochemical characteristics of iron aluminides in the H_2SO_4, H_2SO_4 + KSCN and HCl solutions were investigated using electrochemical tests. The corrosion morphologies in iron aluminides were analysed by utilising optical microscopy. It was found that the addition of Cr and Mo to iron aluminides increased the corrosion potential, pitting potential and repassivation potential. The active current density, passive current density and reactivation current density decreased as Cr and Mo were added. In the case of Mo addition, the passive current density was slightly higher in the H_2SO_4 solution than in solutions containing SCN^- and Cl^-. When B was added to samples, the corrosion potential and repassivation potential decreased, whereas the active current density, passive current density, reactivation current density and pitting potential increased. Iron aluminides containing Mo and Cr showed remarkably improved intergranular and pitting corrosion resistance to SCN^- and Cl^- solution. On the other hand, B addition accelerated granular and intergranular corrosion by precipitation of borides.

1. Introduction

Iron aluminides [Fe_3Al: 28 at % Al] are of considerable interest for low to intermediate temperature structural applications in which low cost, low density and good corrosion or oxidation resistance are required. However, their application is currently limited by their room temperature brittleness. One of the methods being pursued to improve room temperature ductility is the addition of a third element, such as Mn, Cr and Mo, etc. [1,2]. McKamey *et al.* [3] have shown that the ductility of Fe_3Al alloys can be substantially improved by increasing the aluminium content from 25 to 28–30 at % and by adding 2–6 at % chromium. Also the beneficial effect of Cr has been shown mainly to be a result of Cr modifying the surface composition and reducing the susceptibility of the alloy to environmental embrittlement [4]. These Cr-modified alloys can be further improved by thermomechanical treatment and by alloying with Mo and Nb [5].

Regarding the characterization of resistance to aqueous corrosion of the iron aluminides, the only current study is that by Kim and Buchanan [6] who investigated the pitting and crevice corrosion of intermetallics in a mild acid chloride solution. Their work was limited to establishing the role of Mo and Cr of iron aluminides in an acid chloride solution. The present paper aims to reveal the effects of Cr, Mo and B on the corrosion properties of Fe_3Al intermetallics in H_2SO_4, HCl and KSCN solutions by electrochemical methods.

2. Experimental procedure

The chemical compositions of the iron aluminides used are given in Table I. Fe and Al materials were prepared under hydrogen and in a vacuum arc furnace, respectively. The produced materials were heated at 1000 °C under a high purity dried Ar atmosphere and were held at 500 °C for 2 days to stabilize the DO_3 structure of the materials. The specimen used as a working electrode was finished by grinding it on 600-grit silicon carbide paper. A saturated calomel electrode (SCE) and high density carbon electrode were used as a reference and a counter electrode, respectively, and these electrodes were set following ASTM G5-87 [7]. Electrochemical measurement of the samples was accomplished with an EG&G Instruments Model 273 potentiostat connected to a computer system. The potentiodynamic method was carried out in a 0.5 M H_2SO_4 and an electrochemical potentiokinetic reactivation (EPR) test in 0.5 M H_2SO_4 and 0.01 M KSCN solution. For the pitting test, a cyclic

0022–2461

TABLE I Chemical compositions of Fe–28Al system

Materials	Chemical Composition (at %)				
	Al	Cr	Mo	B	Fe
FA	28	–	–	–	72
FAC2	28	2	–	–	70
FAC6	28	6	–	–	66
FACM2	28	2	1	–	69
FACM6	28	6	1	–	65
FAB	28	–	–	0.02	71.98
FACB2	28	2	–	0.02	69.98
FACB6	28	6	–	0.02	65.98

potentiodynamic polarization (CPP) test was performed in 0.5 M HCl solution. After each test, the surface of all samples were observed by optical microscopy.

3. Results and discussion

3.1. Effect of alloying elements on the anodic polarization behaviour

Fig. 1 shows the anodic polarization curves of AISI 316 stainless steel and iron aluminide alloys with different alloying elements in 0.5 M H_2SO_4. The higher transpassive potential for iron aluminides alloys compared to AISI 316 stainless steel in Fig. 1, seems to be due to the formation of aluminium compounds from the solution [8]. Table II summarized the corrosion (E_{corr}), transpassive (E_{trans}) and primary passive (E_{pp}) potentials, critical current density for passivation (I_a) and critical current density for the passive region (I_p) for the tested materials. From Table II, the corrosion potential (E_{corr}) of FA was determined to be of lower value and of higher passive current density in the passive range of potential. As shown in Table II, when compared to 2 at % Cr, 6 at % Cr content increased the corrosion potential and decreased significantly the passive current density. The result might be due to the formation of a passive film composed of $Cr(OH)_3$ and Cr_2O_3 [9].

As can be seen from Table II, the addition of Mo showed a higher corrosion potential and lower active current density in comparison with Cr addition. From the anodic polarization curve (Fig. 1), the slight increase in current density in the passive range of the potential results from Mo dissolved as MoO_4^{2-} in 0.5 M H_2SO_4 solution and the negative charged ion (MoO_4^{2-}) reduces the activity of dehydrogenation and resulted in no passivation with decreasing ratio of $Cr_2O_3/Cr(OH)_3$ [10].

The effect of boron on the anodic polarization behaviour of FAB, FACB2 and FACB6 in 0.5 M H_2SO_4 solution at 25 °C resulted in a lower corrosion potential and higher active and passive current density compared to the results given in Table II.. The added boron would be precipitated as $(Cr, Fe)_2B$ or $(Cr, Fe)_{23}B_6$ suggested by Goldschmidt [11]. It might be suggested that the formation of boride lowers Cr content in the area adjacent to the precipitate and the Cr depleted area near the product is corroded which is generally found in stainless steels (see the microstructure of the corroded surfaces shown in Section 3.4).

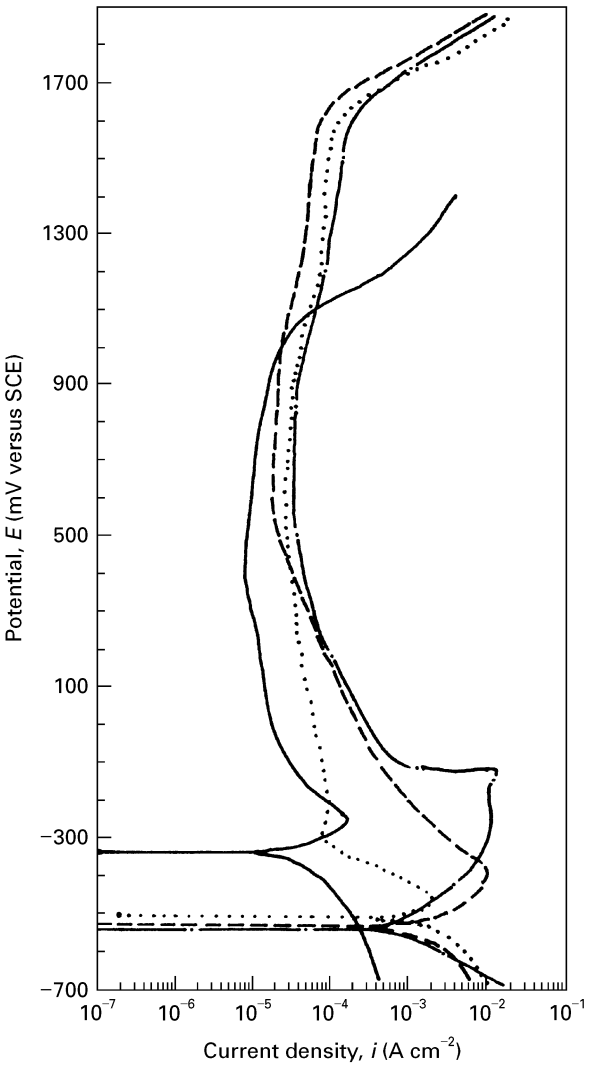

Figure 1 Anodic polarization curves of AISI 316 stainless steel (——), FAC6 (- - -), FACM6 (· · · ·) and FACB6 (–·–) in 0.5 M H_2SO_4 solution at 25 °C.

3.2. Effect of alloying elements on the grain boundary activation

In order to find the degree of sensitization to intergranular attack from a grain boundary activator and to increase the reactivation current density, both a stainless steel and iron aluminides containing different amounts of Cr were investigated using the electrochemical potentiokinetic reactivation method. It was found that the reactivation current density (I_r) is higher than the activation current density (I_a) of iron aluminides, except for FACM2 and FACM6, irrespective of the addition and the amount of alloying elements as shown in Fig. 2. The results suggested that the reaction is very active in grains and at grain boundaries. The degree of sensitization (P_a) (C cm^{-2}) is generally given as

$$P_a = Q/S \quad (1)$$

TABLE II Corrosion (E_{corr}), transpassive (E_{trans}), primary passive potential (E_{pp}), critical current density for passivation (I_a) and critical current density for passive region (I_p) of Fe–28Al intermetallic compounds with alloying elements after anodic polarization measurement in 0.5 M H_2SO_4 solution

Intermetallic compounds	E_{corr} (mV versus SCE)	E_{trans} (mV versus SCE)	E_{pp} (mV versus SCE)	I_a ($A\,cm^{-2}$)	I_p ($A\,cm^{-2}$)
FA	− 550	1650	− 430	1.5×10^{-2}	2.5×10^{-4}
FAC2	− 540	1650	− 300	2.0×10^{-2}	5.0×10^{-5}
FAC6	− 520	1650	− 380	1.0×10^{-2}	2.0×10^{-5}
FACM2	− 510	1620	− 430	3.0×10^{-3}	2.5×10^{-5}
FACM6	− 500	1620	− 430	2.0×10^{-3}	2.0×10^{-5}
FAB	− 550	1650	− 390	2.7×10^{-2}	8.0×10^{-5}
FACB2	− 555	1650	− 400	2.5×10^{-2}	1.0×10^{-4}
FACB6	− 530	1650	− 110	1.0×10^{-2}	4.0×10^{-5}
316SS	− 330	1050	− 250	1.7×10^{-4}	1.0×10^{-5}

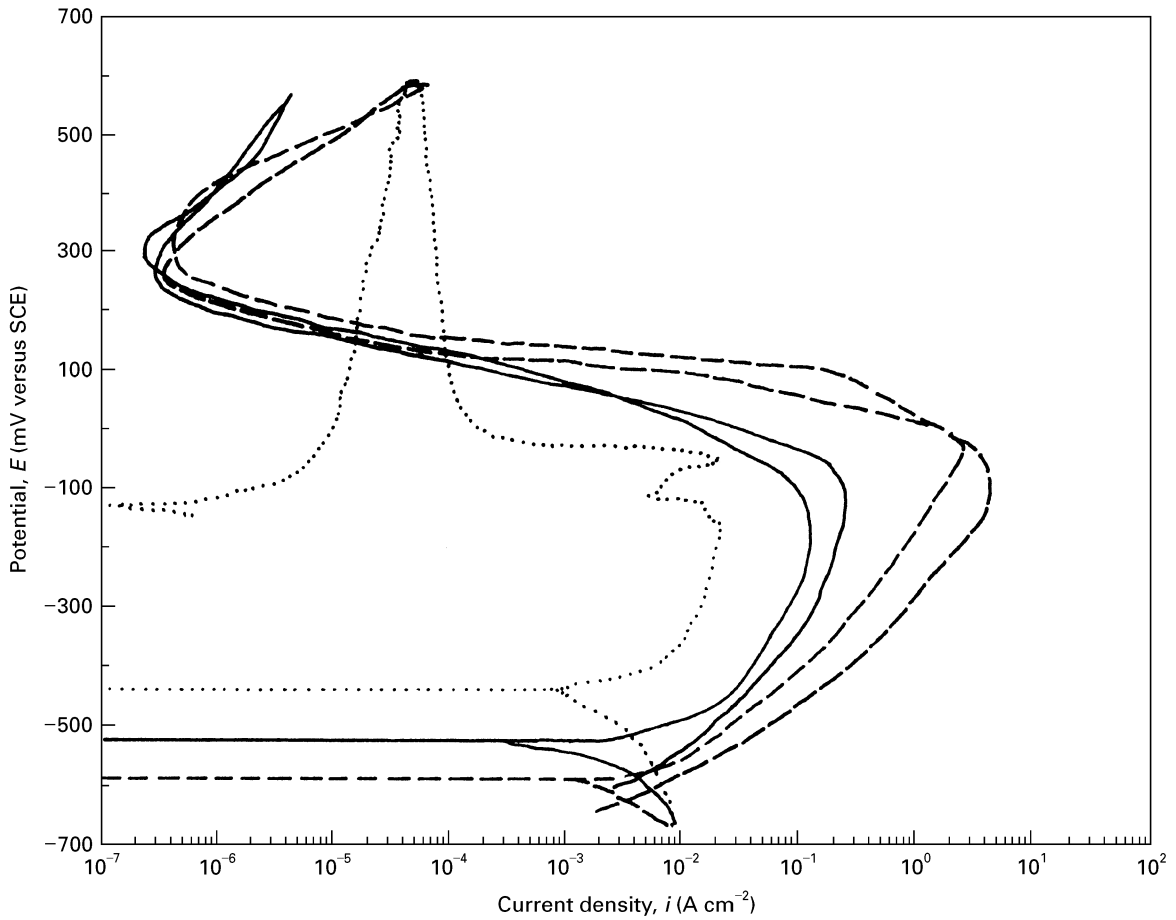

Figure 2 EPR curves of FAC6 (——), FACM6 (· · · ·) and FACB6 (- - -) in 0.5 M H_2SO_4 + 0.01 M KSCN solution at 25 °C.

where Q is the total charge measured and S, the total grain boundary area, is given as

$$S = A\{5.0954 \times 10^{-3} \exp(0.3496X)\} \quad (2)$$

where A is the area of the specimen and X is the ASTM grain size number determined at magnification of 100 times.

The total quantity of electronic charge, Q, is related to the area surrounded by the reactivation curve (under the potential against the current curve) of the EPR test, so that P_a ($C\,cm^{-2}$) was obtained [12, 13]. Assuming that S from Equation 2 is the same for all the samples used in this study, the area of reactivation of the EPR test for iron aluminides was ranked in order of area, FA > FAC2 > FAC6. From these results (Table III), it is apparent that the addition of Cr into FA prevented corrosion from SCN^- solution. In comparison, considering the higher content of Cr to Fe, the solution-treated AISI 316 stainless steel showed the lower I_r and I_a values, which means that the grain boundaries are more stable in SCN^- solution.

Table IV shows the data obtained from EPR measurements of iron aluminides containing Cr, Mo and B, respectively, in 0.5 M H_2SO_4 + 0.01 M KSCN solution. From these results and Fig. 2, the activation current density of FACM is very similar to that of stainless steel, but the reactivation was not found. This

TABLE III The degree of sensitization of intergranular attack of iron aluminides

Test specimens	ASTM grain size number	Q(C)	P_a(C cm^{-2})
FA	2.01	68.9	6755
FAC2	2.01	60.1	5882
FAC6	2.01	50.3	4931
FAB	2.81	69.0	5000
FACB2	2.81	63.7	4616
FACB6	2.81	62.7	4543
316SS	5.23	7.9	258

TABLE IV Primary passive potential, maximum current density for passivation and maximum current density for reactivation of Fe–28Al intermetallic compounds with alloying elements after EPR measurement in 0.5 M H_2SO_4 + 0.01 M KSCN solution

Intermetallic compounds	E_{pp} (mV versus SCE)	I_a (A cm^{-2})	I_r (A cm^{-2})
FA	120	3.0×10^{-1}	0.13×10^{1}
FAC2	30	1.8×10^{-1}	8.0×10^{1}
FAC6	− 150	1.2×10^{-1}	1.8×10^{1}
FACM2	− 160	1.0×10^{-1}	NR[a]
FACM6	− 180	2.0×10^{-2}	N.R.
FAB	60	0.8×10^{1}	1.0×10^{1}
FACB2	− 20	0.25×10^{1}	0.4×10^{1}
FACB6	− 50	7.0×10^{-1}	0.12×10^{1}
316SS	− 200	1.3×10^{-3}	7.0×10^{-4}

[a] NR: no reactivation.

might be due to the addition of Mo, which existed as MoO_4^{2-} in the electrolyte solution and acted as a corrosion inhibitor against SCN^- in order to form the passivation. The effect of B addition to iron aluminides induced a decrease in the corrosion potential, and increase in the activation and reactivation current density which was related to the increasing amount of boride in the grains and at the grain boundaries.

3.3. Effect of alloying elements on the pitting behaviour

Table V shows the data measured from cyclic potentiodynamic polarization (CPP) tests for iron aluminides with added Cr, Mo and B, respectively, in 0.5 M HCl solution. As shown in Table V, as with increasing the amount of Cr, the corrosion potential increased relative to the content, FAC6 > FAC2 > FA. These results, pitting potential obtained with the CPP test, were in good agreement with Kim and Buchanan's data [6]. The addition of Cr accelerated the formation of the passive film, which protected against attack by Cl^- and resulted in increased corrosion resistance. Cr prevents pitting entirely in the passive potential range. The repassivation potential of FA not containing Cr was measured as nil and increased as the content of Cr increased: − 290 and − 260 mV for 2 and 6 at % Cr, respectively.

The pitting corrosion resistance in Table V was improved by adding Mo, which increased the pitting and repassivation potential compared with the case

TABLE V Corrosion, pitting and repassivation potential values of Fe–28Al intermetallics with alloying elements after CPP tests in 0.5 M HCl solution

Intermetallic compounds	E_{pit} (mV versus SCE)	E_{rep} (mV versus SCE)	E_{corr} (mV versus SCE)
FA	− 200	ND[a]	− 525
FAC2	− 110	− 290	− 515
FAC6	− 70	− 260	− 485
FACM2	10	− 225	− 450
FACM6	40	− 200	− 420
FAB	− 170	ND[a]	− 515
FACB2	− 150	− 300	− 510
FACB6	− 60	− 270	− 485

[a] ND: not defined.

not containing Mo. Thus, the addition of Mo to iron aluminides containing Cr had a synergistic effect on the pitting resistance of Fe_3Al. The increasing pitting potential with the addition of Mo is explained by two mechanisms. One is the ion selectivity of the passive film composed of MoO_4^{2-} on the specimens in acidic solution. The MoO_4^{2-} anions play an important role in preventing ingress of Cl^- ions on the passive film [14]. The second is that after the reaction with HCl solution, Mo forms MoO_2Cl and MoO_3 as a protecting film on the specimen surface [15]. On the other hand, the addition of B resulted in a lower E_{corr}, and a slightly lower pitting and reactivation potential compared to those of boron-free specimens as shown in Table V. This is due to the influence of $B_4O_7^{2-}$ formed by dissolving from the matrix into the solution, which then acted as a pitting inhibitor against Cl^- in the solution [16].

3.4. Observation of surface morphology after each corrosion test

Fig. 3 shows optical micrographs of the corrosion behaviour of iron aluminides containing Cr, Mo and B, respectively, in H_2SO_4. FA not containing Cr appeared to be severely corroded, in that the surface, as shown in Fig. 3a, had an unstable corrosion morphology. While, in Fig. 3b the corrosion of FAC6 was less active than on FA because of the formation of a passive film on the material. By adding Mo, FACM6 showed a strong corrosion resistance against SO_4^{2-} attack. In the case of the addition of B, however, FACB6, shown in Fig. 3d, was found to have proper corrosion resistance compared to Fig. 3b.

In H_2SO_4 solution containing SCN^- the morphology of the surface of materials after EPR tests are shown in Fig. 4. The effect of SCN^-, as an activator to increase the reactivation current density on corrosion behaviour, was clearly seen through Fig. 4a to d. In Fig. 4a, FA was found to be severely corroded on the surface of the grains and can explain the increasing activation and reactivation current density compared to those of stainless steel. FAC6 including Cr showed less corrosion in the whole area of the grains owing to the formation of a passive film and FACM6 with Mo kept a clean surface by protecting from attack by

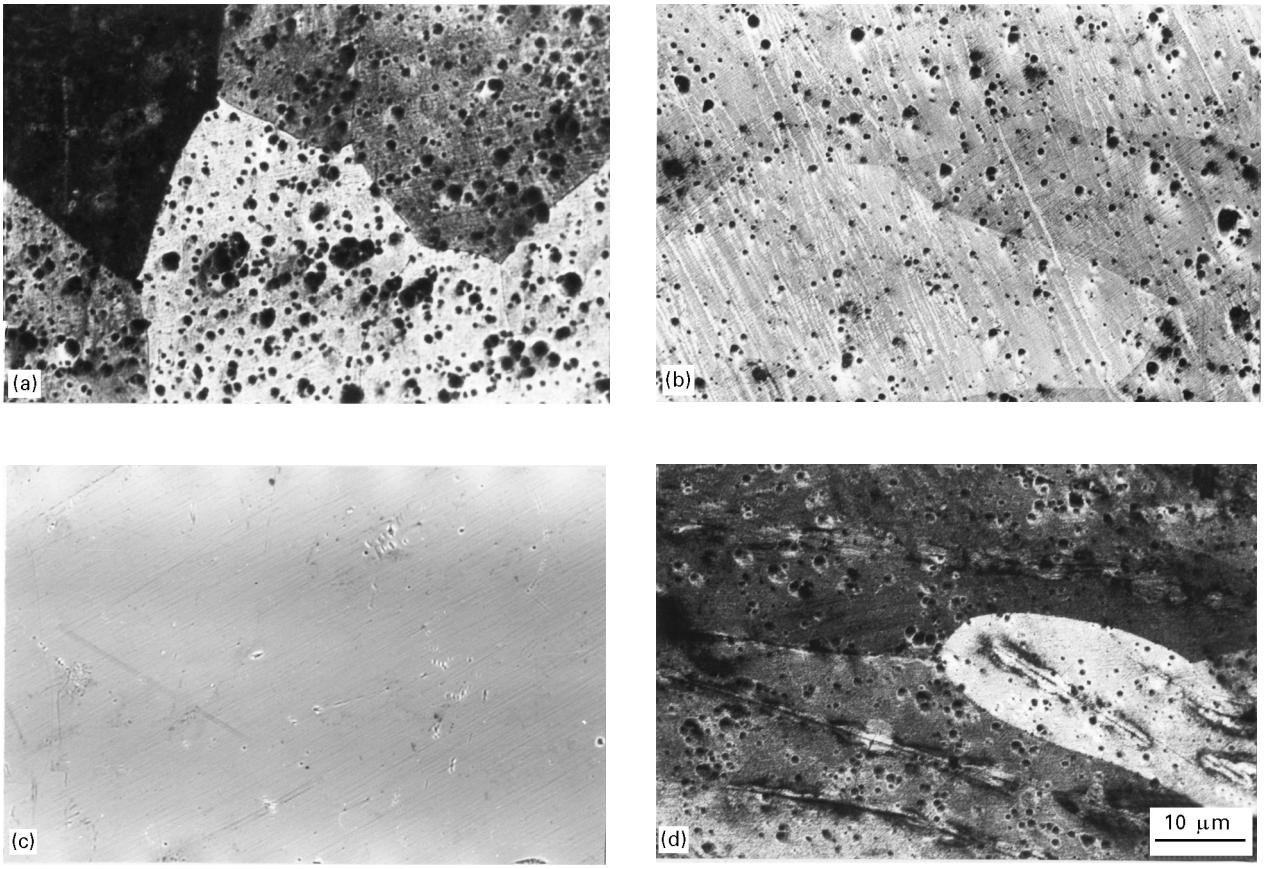

Figure 3 Optical micrographs showing corrosion behaviour of iron aluminides after a corrosion test in 0.5 M H_2SO_4 solution at 25 °C: (a) FA, (b) FAC6, (c) FACM6 and (d) FACB6

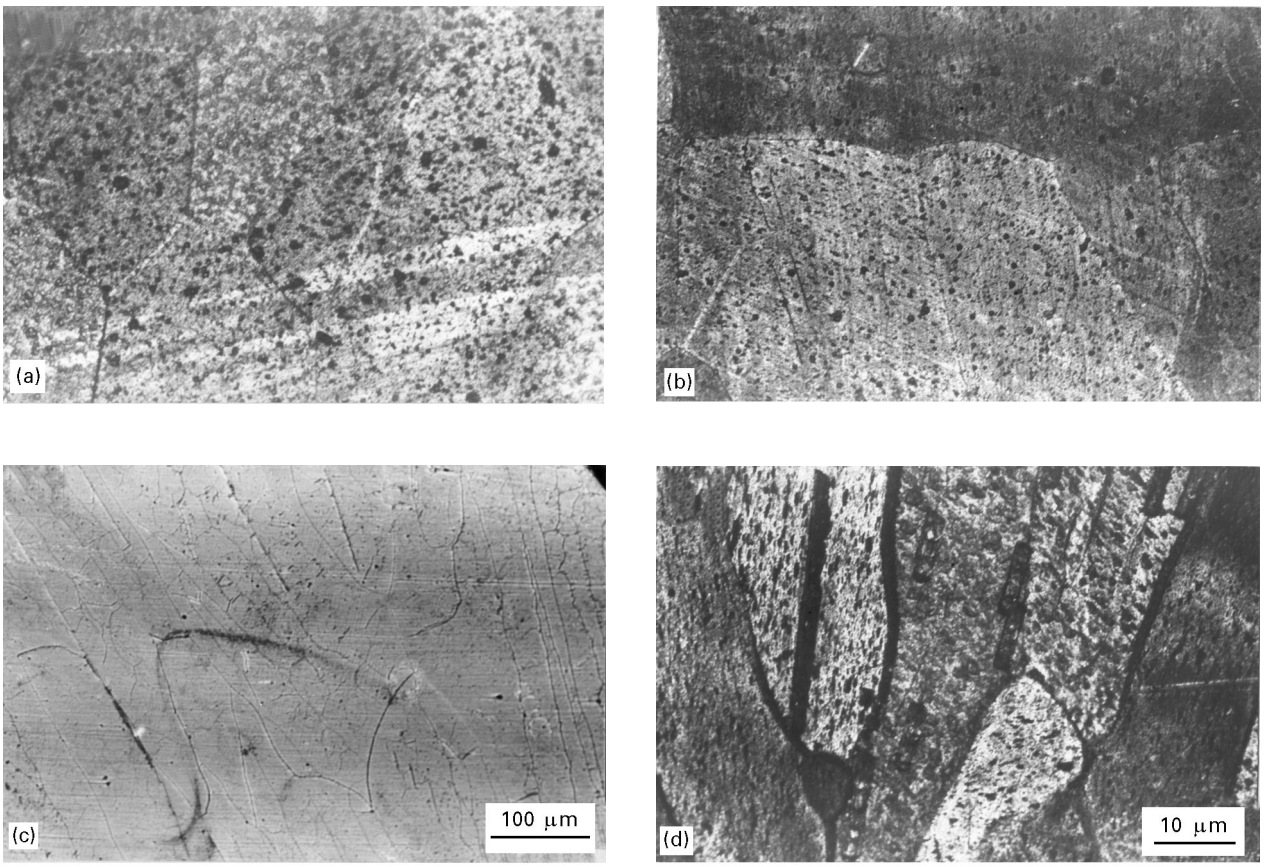

Figure 4 Optical micrographs showing corrosion behaviour of iron aluminides after a EPR test in 0.5 M H_2SO_4 + 0.01 M KSCN solution at 25 °C: (a) FA, (b) FAC6, (c) FACM6 and (d) FACB6

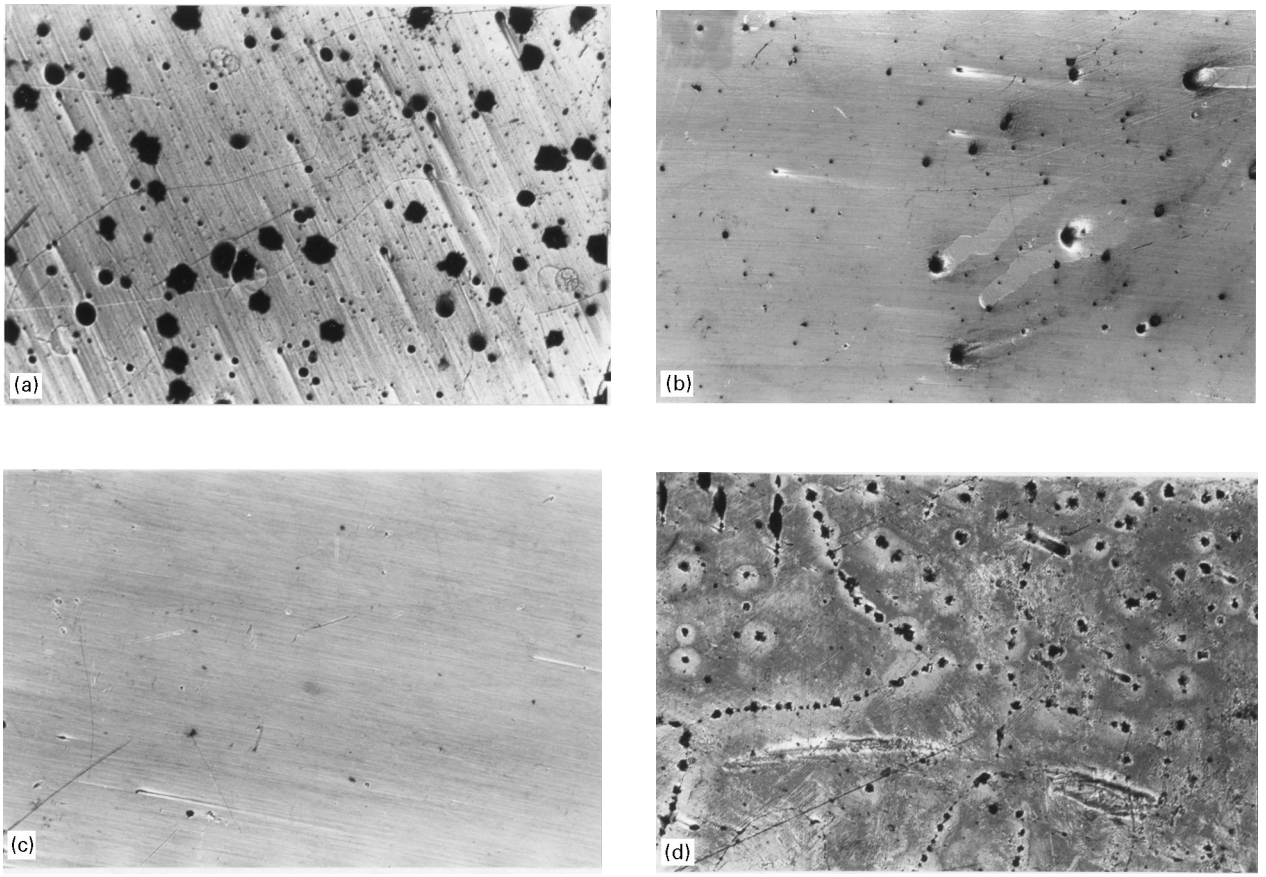

Figure 5 Optical micrographs showing corrosion behaviour of iron aluminides after a CPP test in 0.5 M HCl solution at 25 °C: (a) FA, (b) FAC6, (c) FACM6 and (d) FACB6

aggressive anions such as SCN^- and Cl^- by forming MoO_4^{2-})[17, 18]. In fact, the SCN^- is known to be an anion that forms pits as well as being a grain boundary activator in the solution. FACB6 containing boron after corrosion tests was observed as shown in Fig. 4d, in which borides, formed at the grain boundaries, were strongly attacked by SCN^-, and thus exhibited intergranular corrosion.

Fig. 5a–d shows micrographs of corrosion of iron aluminides in chloride acid solution. Many pits, caused by Cl^- were observed in FA (Fig. 5a), and the number of pits was reduced for FAC6 (Fig. 5b), and hardly present in FACM6 containing Mo (Fig. 5c). It is thought that Mo reacts with Cl^- first and then forms MoO_2Cl, MoO_2 and MoO_3 compounds [6] on the surface of FACM6. Fig. 5d shows the effect of boron in FACB6 showing that severe attack only occurs at the grain boundary because boron is first dissolved in the matrix forming $B_4O_7^{2-}$, and then it acts as a pitting corrosion inhibitor against Cl^- attack [16].

4. Conclusion

1. Adding Cr to Fe_3Al increased the corrosion potential and significantly decreased the active and passive current density. In the case of addition of Mo, the result is the same as adding Cr except for a slight increase in passive current density. On the other hand, the addition of B showed totally opposite results to those observed in Fe_3Al containing Cr.

2. The effect of alloying elements on the grain boundary activity (intergranular attack) was found to be an increase in the degree of sensitization, ranked in the order of addition of Fe_3Al Mo > Cr > B.

3. The CPP tests are strongly affected by the alloying elements. Cr addition increased the corrosion, pitting and repassivation potential and Mo additions had a greater effect on each of the potentials. In contrast boron addition slightly reduced the pitting and repassivation potential in comparison with Cr and Mo addition to Fe_3Al.

4. The observation of surface morphology after corrosion tests showed that the Fe_3Al containing Cr and Mo had far fewer pits than that containing boron.

Acknowledgements

The authors acknowledge the support of the Korea Pohang Steel Company (POSCO).

References

1. B. SCHMIDT, P. N. NAGPAL and I. BAKER, in High Temperature Ordered Intermetallic Alloys III, Mat. Res. Soc. Symposia Proceedings, Vol. 133 (MRS, 1989) p. 755.
2. P. F. TORTORELLI and J. H. DEVAN, *Mater. Sci. Eng.* **A153** (1992) 573.
3. C. G. MCKAMEY, J. A. HORTON and C. T. LIU, *J. Mater. Res.* **4** (1989) 1156.
4. J. R. KNIBOLE and R.N. WRIGHT, *Mater. Sci Eng.* **A153** (1992) 382.
5. N. S. STOLOFF and C.T. LIU, *Intermetallic* **2** (1994) 875.

6. J. G. KIM and R. A. BUCHANAN, *Corrosion* **50** (1994) 658.
7. ASTM Wear and Erosion, Metal Corrosion, section 3, Vol. 03.02, (American Society for Testing and Materials, Philadelphia, PA, 1988) p. 97.
8 M. POURBAIX, "Atlas of Electrochemical Equilibria in Aqueous Solutions" (Pergamon Press, London, 1966) p. 168.
9. Z. SZKLASKA-SMIALOWSKA, "Pitting Corrosion of Metals" (NACE, Houston, 1986) pp. 218, 147.
10. C. R. CLATON and Y. C. YU, *J. Electrochem. Soc.* **133** (1986) 2465.
11. GOLDSCHMIDT, H. J., *J. Iron Steel Inst. Lond.* **209** (1971) 900.
12. W. L. CLARKE, R. L. COWAN and W. L. WALKER ASTM STP 656 (American Society for Testing and Materials, Philadelphia, PA, 1978) pp. 99.
13. D. A. JONES, "Principles and Prevention of Corrosion" (Maxwell MacMillan Eds., New York, 1992) p. 302.
14. M. SKASHITA and N. SATO, *Corros. Sci.* **17** (1977) 473.
15. C. L. ROLLINSON, "The Chemistry of Chromim, Molybdenum and Tungsten" (Pergamon Press, Oxford, 1975).
16. I. L. ROZENFELD, "Corrosion Inhibitors" (McGraw-Hill, New York, 1981) p. 174.
17. A. P. MAJIDI and M. A. STREICHER, *Corrosion* **40** (1984) 393.
18. R. C. NEWMAN, H. S. ISAACS and B. ALMAN, *ibid.* **38** (1980) 261.

Received 19 January
and accepted 17 September 1996